Mat. Res. Bull., Vol. 22, pp. 1249-1257, 1987. Printed in the USA.
0025-5408/87 $3.00 + .00

HIGH PERFORMANCE NITRIDE MATERIALS RESEARCH IN THE CHINESE ACADEMY OF SCIENCES

Dongsheng Yan (T.S. Yen)

The Chinese Academy of Sciences
Beijing, CHINA

ABSTRACT

The paper deals with the phase relationships of nitride ceramics, which are relevant to compositional optimization, oxidation resistance, post-sintering heat-treatments, the role of rare earth oxide additives, and fracture toughness.

MATERIALS INDEX: nitrides, silicon, aluminum, yttrium, oxides

Nitride ceramics are one of the main families of high performance inorganic materials that have attracted a great deal of worldwide attention. The Chinese Academy of Sciences has been pursuing nitride ceramics research for more than a decade (1-5). Research efforts have been focused on the understanding of the phase equilibrium relationship of multi-component systems, phase composition manipulation and grain boundary engineering, etc., in order to develop improved materials with fine and uniform microstructure with advanced properties.

1. Critical review and revisions of phase relationships relevant to compositional optimization.

Additives are necessary to sinter silicon nitride materials because of the highly covalent nature of the chemical bonds. The fundamental phase relationship of the Si, Al/O, N system has been studied by Jack (6) and Gauckler *et al.* (7) (Fig. 1). These studies indicated the importance of forming β-Si_3N_4 solid solution (β's.s.) maintaining a M/X ratio of 3/4 and having the general formulae of $Si_{6-z}Al_zO_zN_{8-z}$. They also showed the very limited solid solution of Si_2N_2O with Al_2O_3 (O's.s.) with M/X ratio of 2/3.

It has also been shown both in our lab and elsewhere that that Y_2O_3 and Al_2O_3 are effective additives for producing better material, especially for high temperature applications. Naik and Tien (8) have studied the Si, Al, Y/O, N system and asceratined an important compatible region of $Y_2O_3 \cdot 2SiO_2$ with β's.s. and O's.s. (Fig. 2). Critical reviews and studies of Si, Al/O, N and Si, Al, Y/O, N systems have been intensively carried out both in our laboratory and in close collaboration with other laboratories. A number of important features have been uncovered and revisions suggested. Some of the new things that will be important for the designing and development of advanced materials are:

(1) The garnet phase is compatible to β-Si_3N_4 and β's.s. (Fig. 3).
(2) β-Si_3N_4 and O's.s. are compatible, and there should be a tie line

between them as shown by the study of Si_2N_2O-Al_2O_3-Y_2O_3 (La_2O_3 or CaO) system (10) (Fig. 4). O's.s. can dissolve up to 15 m/o of Al_2O_3 with the general formulae of $Si_{2-x}Al_xN_{2-x}O_{1+x}$ up to x=0.3, which is compatible with β's.s. up to z=0.8 (Fig. 5). Thus the phase diagram of Si, Al/O, N system should be revised.

(3) From what we can see from Fig. 4, β-Si_3N_4-O's.s.-YAG-H form a compatible region <1550°C. If it is heated up to 1700°C and annealed at 1200-1300°C, H phase decomposes and the compatible region becomes β-Si_3N_4-O's.s.-YAG-Y2S.

(4) Si, Al, Y/O, N phase relationship should be revised as Fig. 6 and Fig. 7. The most important of which is the compatibility of the garnet phase with silicon nitride - β 's.s.-O's.s. phases, the compatibility of the yttrium disilicate phase with silicon nitride-silicon oxynitride-O's.s. phase and the possible coexistence of garnet with yttrium disilicate phases with Si_3N_4-O's.s., depending on composition. Materials with promising properties within these regions can be and have been tailored by phase compositional manipulation and grain boundary engineering.

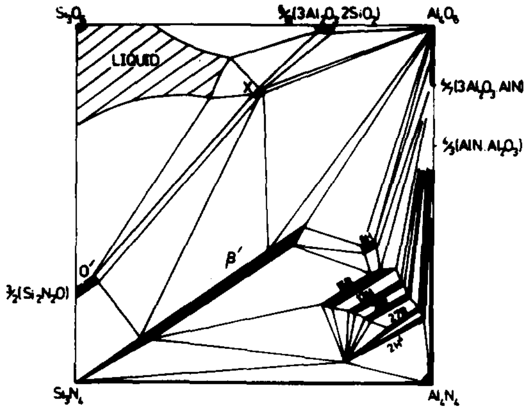

FIG. 1

Behaviour diagram for the Si-Al-O-N system at 1700°C, after Jack.

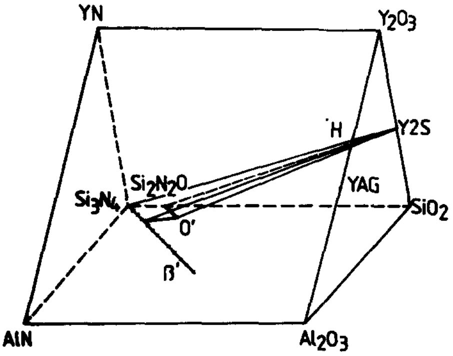

FIG. 2

The compatibility tetrahedron Si_2N_4-Si_2N_2O- $β'_{10}$-O'-$Y_2Si_2O_7$, after Naik et al.

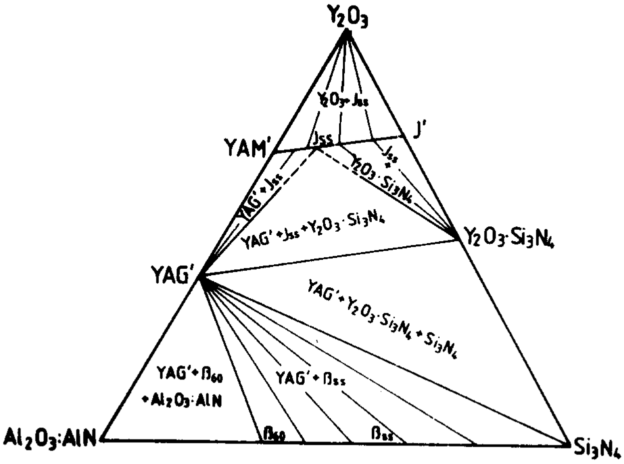

FIG. 3

Subsolidus phase diagram of the system Y_2O_3-Al_2O_3:AlN-Si_3N_4.

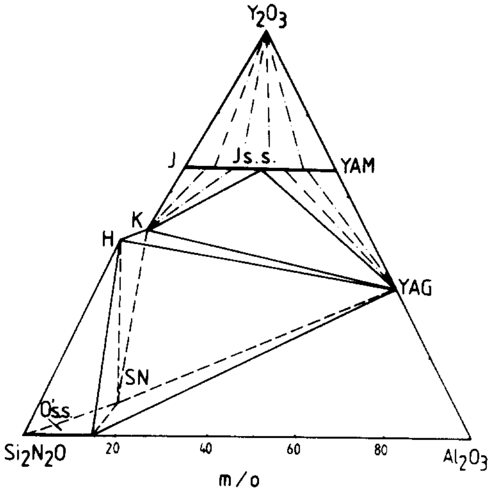

FIG. 4

Subsolidus phase diagram of the Si_2N_2O-Al_2O_3-Y_2O_3 system. J=$2Y_2O_3 \cdot Si_2N_2O$; SN=Si_3N_4; YAM=$2Y_2O_3 \cdot Al_2O_3$; K=$Y_2O_3 \cdot Si_2N_2O$; H=$Y_{10}(SiO_4)_6N_2$; YAG=$3Y_2O_3 \cdot 5Al_2O_3$.

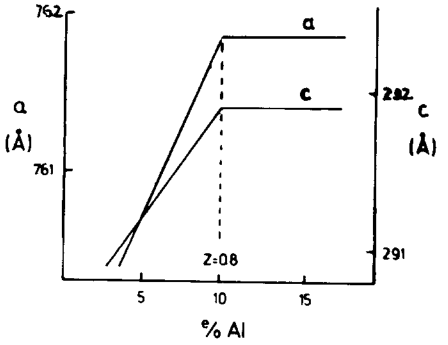

FIG. 5

Variation of cell dimension of β' coexisting with O's.s. of x=0.3; limit of β', z=0.8.

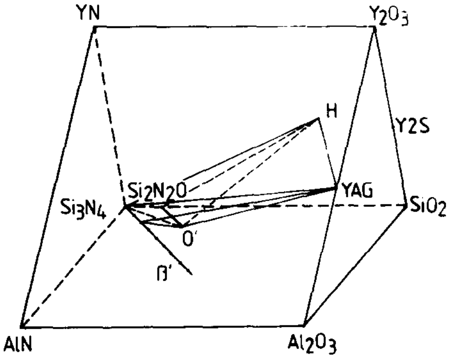

FIG. 6

Phase relationships of O'- β' in Y-Si-Al-O-N system at 1550°C.

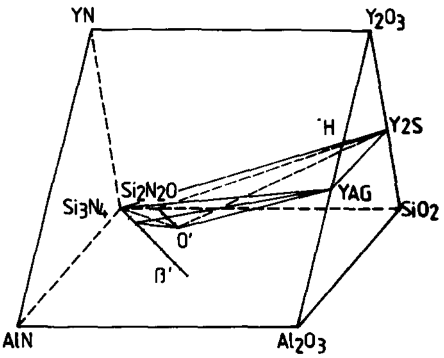

FIG. 7

Phase relationships of O'-β' in Y-Si-Al-O-N system at devitrifying temperature 1200-1300°C.

2. O'-β' composite sialons-processing and oxidation resistance.

From the studies mentioned above, the tailoring of β's.s.-O's.s. composites with garnet or yttrium disilicate or both as grain boundary phases is possible. Both garnet and yttrium disilicate are refractory. And the combination of the good mechanical properties of β' and oxidation resistance of O' can tailor good engineering materials with a fair degree of freedom. Compositions have been prepared within these regions (11), as shown in Fig. 8, on the Si-Al-O-N plane leaving out the yttria added in additional. It may be sufficient to mention that compositions within the top triangle are richer in O's.s. content with yttrium disilicate as the grain boundary phase. While compositions within the lower triangle are richer in β's.s. content with garnet as the grain boundary phase. And those close to the Si_3N_4-O's.s. (x=0.3) line will have both garnet and disilicates depending on composition and heat treatment. Heat treatment has a great deal to do with the appearance of grain boundary phases. Comparing the oxidation resistance of compositions 6, 3 and 7, it can be seen that composition 6, which is an O's.s. based material, is better than composition 7, which is a β's.s. based material. Moreover, heat treatment schedule is very important. These are evident in Fig. 9. SEM and EDAX analysis indicates that the major oxidation products are cristobalite and γ -$Y_2Si_2O_7$. There is obviously considerable room for tailoring O'-β' sialon composites, as far as oxidation resistance and also mechanical properties are concerned. The optimization of these composites may lead to promising materials for different purposes.

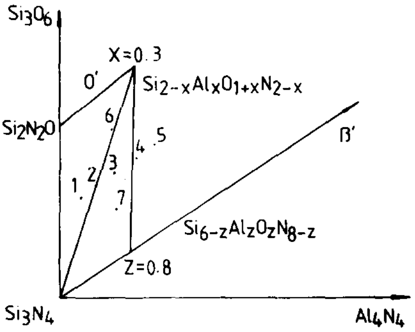

FIG. 8

Compositions explored in the O'-β' region of Si-Al-O-N system (11).

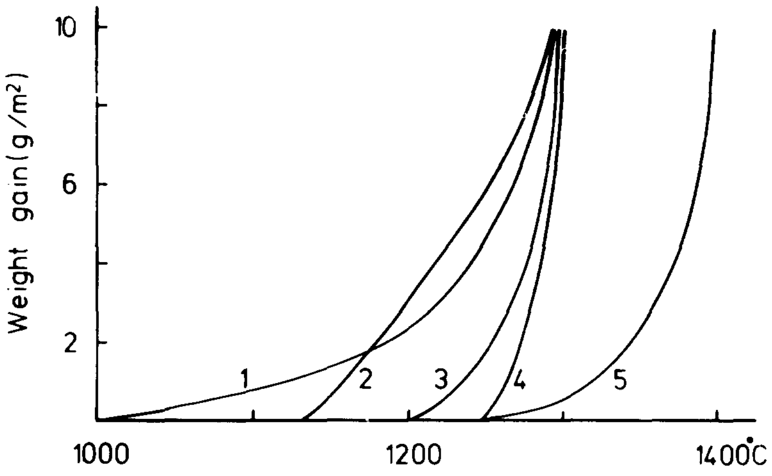

FIG. 9

Oxidation after 48 hrs at each temperature in the range 1000-1400°C (11).
Composition 3: curve 1 - without devitrification
curve 3 - devitrification at 1200°C for 16 hr
curve 5 - devitrification by a stepwise heat treatment
Composition 6: curve 4 - devitrification at 1200°C for 16 hr
Composition 7: curve 2 - devitrification at 1200°C for 16 hr

3. RBSN post-sintered and heat treated.

β' sialon material with refractory grain boundary phases has been developed through post-sintering reaction bonded silicon nitride (RBSN) route plus proper heat treatment (12). The advantage of lower sintering shrinkage of reaction bonded material and thus the possibility of making ocmplex shapes with better dimensional accuracy has also attratced much attention (13-15). The reaction bonded material was processed with the incorporation of Y_2O_3, Al_2O_3 and AlN. The phase compositions of the reaction bonded, post-sintered and heat treated (or annealed) materials as determined by XRD and HREM techniques are shown in Table I. Figures 10 and 11 are transmission electron micrographs which show the crystallization of YAG from glassy phase at grain boundaries or at triple points between β' and α' grains. The remaining glassy phase after crystallization is rather difficult to find under TEM.

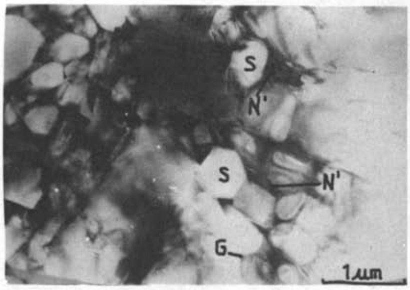

FIG. 10

TEM of post-sintered RBSN without heat treatment: S - β' or α' grains; N' - Y_2SiAlO_5N; G - glassy phase.

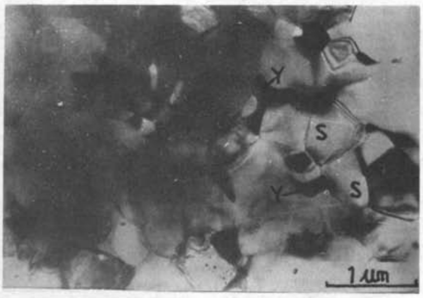

FIG. 11

TEM of post-sintered RBSN in the heat treated condition, Y - YAG.

TABLE I

Phases Composition Changes of RBSN at Various Processing Stages

	After reaction sintering	Sintered at 1800°C	After heat treatment
Main Phase	β'	β'	β'
Secondary Phase	α	α'	α'
Minor Phases	YAG	N' Glass	YAG
Trace	AlN	Y_2SiO_5 J	J_{ss} $Al_{2.83}O_{3.5}N_{0.5}$

N'-Y_2SiAlO_5N, J_{ss}-Solid solution between J & YAM phases

The phase composition and microstructural changes of this composite material along with processing have a significant bearing on the mechanical properties (Table II and Fig. 12). It is noteworthy to point out that their high temperature mechanical strength can be maintained up to about 1400°C.

TABLE II

Physical Properties of Post-Sintered RBSN at Various Processing Stages

Properties	RBSN	Post-sintered at 1800°C	Heat treated at 1450°C
Bulk density g/cm^3	2.63	3.14	3.10
App. porosity, %	15.3	0.58	0.39
Bend strength MPa			
R.T.	247±17	465±44	446.32
1200°C	-	454±14	485±18
1400°C	-	206±17	439±61
K_{Ic} MPa$\sqrt{m}$	3.40±0.17	4.52±0.36	4.77±0.26
Hv kg/cm^2	-	876	1103

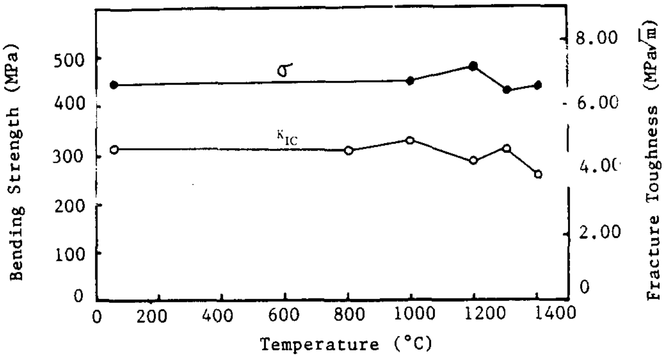

FIG. 12

Strength and fracture of post-sintered and heat-treated RBSN vs temperature.

4. Silicon nitride with rare earth oxide additives.

Rare earth oxide additives are also promising to develop high performance silicon nitride materials with higher levels of strength and fracture toughness up to 1300°C. SI_3N_4 ceramics with Y_2O_3 and La_2O_3 additives have the most impressive high temperature mechanical properties (Fig. 13). The microstructure of this material is composed of fine β-Si_3N_4 grains with α-Si_3N_4 whiskers and an La-containing crystalline material. The role of such a microstructure to enhance high temperature strength and fracture toughness will be explored in the next section.

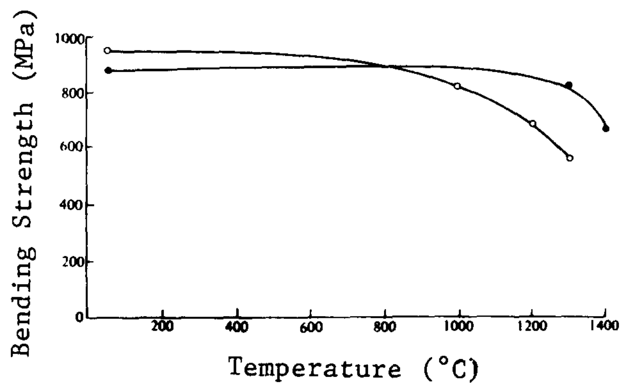

FIG. 13

Strength of HRSN vs temperature; o with Al_2O_3 additive, ● with La_2O_3 additive.

5. Fracture toughness of silicon nitride materials.

The change of fracture toughness with temperature is of considerable concern for materials that are intended for high temperature usage (Fig. 14). Our studies on these materials give a preliminary insight into this problem (16). The microstructures of material A with La_2O_3 addition tested at high temperatures are particularly interesting and are shown in Figs. 15 and 16.

It is interesting to discuss a little more the high fracture toughness (around 9 MPa$\sqrt{m}$ up to 1300°C) of the material with an additional doping with La_2O_3. Uniformly distributed La-containing tetragons, as identified by electron microprobe, usually project out from the matrix of the fratured surface (Fig. 16). This phenomenon strongly suggests that cracks do not propagate through these crystals and go around them, thus they are virtually pulled out from the opposite fracture surface. Microcracks are quite difficult to run through these crystals and are forced to divert their running directions, and thus strengthen the material as a whole. The "pull out" effect will also increase the fracture energy as verified by the experimental results.

For the exploitation of mid-term and long-term applications, several ceramic components made from these materials have been fabricated and gone through testing as important parts in diesel engines for a period of 200 to 1000 hours.

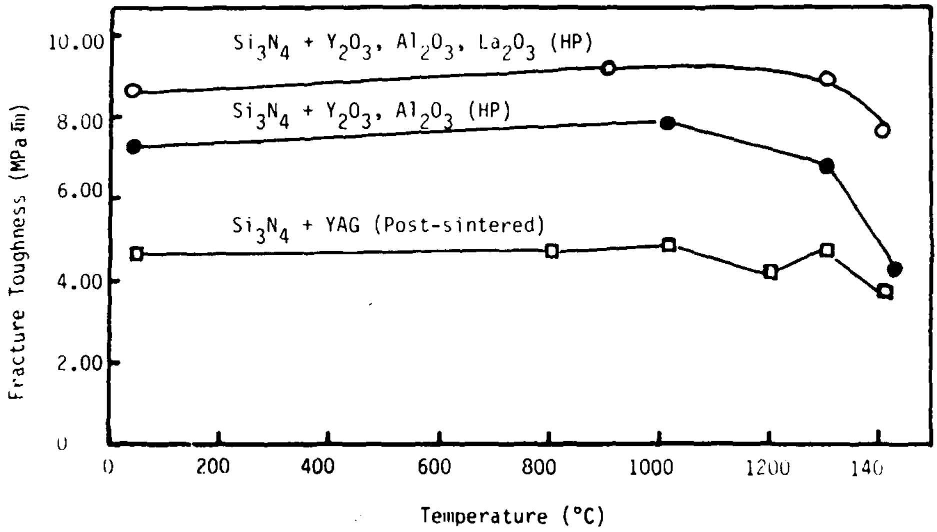

FIG. 14

Fracture toughness vs temperature for silicon nitride ceramics.

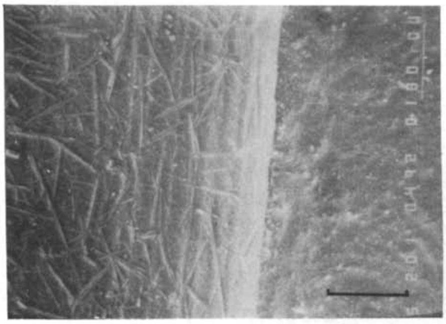

FIG. 15

Scanning electron micrograph for the fracture surface (right) and the notch surface (left) of specimen A after fracture toughness testing at 1400°C (bar=100 μ). (Note the extensive cristobalite formation at the notch surface.)

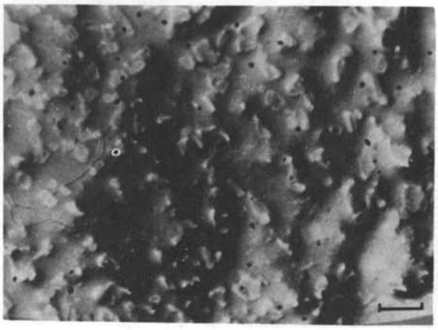

FIG. 16

Enlarged micrograph for the fracture surface of specimen A (bar= 10 μ), showing some of the details of the microstructure.

References

1. T.S. Yen (D.S. Yan), Inorganic New Materials Research and Materials Science, J. Chinese Silicate Soc. 6, 85 (1978).

2. T.S. Yen, Progress of Inorganic Materials Res.: Structure-Property Rela-

tionship of Inorganic Materials Viewed from Different Microstructural Levels, Invited Lecture at the 50th Annual Meeting of the Chinese Chemical Society, 1978, Proceedings of the Chinese Chemical Society (1980).

3. T.S. Yen, Proceedings of CIMTEC IV, Saint Vancent, Italy (1979), published in 1980.
4. T.S. Yen, Progress of Ceramic Research in the Shanghai Institute of Ceramics, Academia Sinica, Ceramics International 7, 1 (1981).
5. T.S. Yen, An Overview of Chinese Research on Processing, Microstructure, and Properties of New Ceramic Materials, 1st China-U.S. Seminar on Ceramic Materials, May 17-21, 1983, Proceedings, 1-35 (1984).
6. K.H. Jack, Proc. Brit. Ceram. Soc. 28, 295 (1979).
7. L.J. Gauckler, H.L. Lucas and G. Petzow, J. Am. Ceram. Soc. 58(7-8), 346 (1975).
8. T.K. Naik and T.Y. Tien, J. Am. Ceram. Soc. 62(11-12), 642 (1979).
9. W.Y. Sun, et al., Trans. Brit. Ceram. Soc. 82, 173 (1983).
10. G.Z. Cao, Z.K. Huang, X.R. Fu and T.S. Yen, Int. J. High Technology Ceramics 1(2), 119 (1985).
11. W.Y. Sun, D.P. Thompson and K.H. Jack, The Fabrication of Composite O'-Sialon Ceramics, in Proc. 21st University Conference on Ceramic Science, The Pennsylvania State University, 1985 (to be published).
12. H.R. Zhuang et al., Proceedings of Symposium on Ceramic Components for Engines, Hakone, October 17-21, 1983; printed 368 (1984).
13. J.A. Mangels and G.J. Tennenhouse, Am. Ceram. Soc. Bull. 59, 1216 (1980).
14. A. Giachello and P. Popper, Ceram. International 5, 110 (1979).
15. M. Bohmer and J. Heinrich, "Keramische Komponenten für Fahrzeng Gasturbinen II", Springer Verlag (1981), p. 517.
16. Y.R. Xu et al., "Silicon Nitride Ceramics with High Fracture Toughness at Elevated Temperatures", Shanghai Institute of Ceramics (1985), to be published.